

ATP Citrate Lyase is a General Tumour Biomarker and Contributes to the Development of Cutaneous Squamous Cell Carcinoma

Ruiting LUO^{1#}, Yingjian HUANG^{1#}, Ruimin BAI¹, Meng LIU¹, Liang SUN¹, Xiaofei WANG² and Yan ZHENG¹

¹Department of Dermatology, the First Affiliated Hospital of Xi'an Jiaotong University, Xi'an, China and ²Biomedical Experimental Center, Xi'an Jiaotong University, Xi'an, China

[#]These authors contributed equally.

ATP citrate lyase, the first rate-limiting enzyme in *de novo* lipogenesis, plays a crucial role in tumour progression. This study explores ATP citrate lyase's potential as a tumour biomarker and its role in cutaneous squamous cell carcinoma. ATP citrate lyase expression patterns were analysed using TCGA and TIMER databases, and patient skin specimens were collected for immunohistochemistry to determine ATP citrate lyase levels. Cell proliferation, cell cycle, apoptosis, and c-Myc expression were assessed in A431 and SCL-1 cells. Stable cell lines with reduced ATP citrate lyase expression were obtained and subcutaneously implanted into nude mice to evaluate *in vivo* tumour growth. Ki67, c-Myc expression and TUNEL staining were analysed in subcutaneous tumours. ATP citrate lyase exhibited upregulation in various tumours, and showed significant associations with prognosis and immune infiltration. Moreover, ATP citrate lyase was highly expressed in cutaneous squamous cell carcinoma. After ATP citrate lyase silencing, cutaneous squamous cell carcinoma cell growth decelerated, the cell cycle halted, cell apoptosis increased, and c-Myc expression decreased. Animal experiments revealed that, following ATP citrate lyase knockdown, tumour tissue growth slowed down, and there was a reduction in Ki-67 and c-Myc expression, accompanied by enhanced TUNEL staining. In conclusion, ATP citrate lyase may serve as a tumour biomarker. It is highly expressed in cutaneous squamous cell carcinoma and may serve as a therapeutic target.

Key words: ATP citrate lyase; biomarker; skin neoplasms.

Submitted Oct 15, 2023. Accepted after review Mar 5, 2024

Published Apr 8, 2024. DOI: 10.2340/actadv.v104.23805

Acta Derm Venereol 2024; 104: 23805.

Corr: Xiaofei Wang, Biomedical Experimental Center, Xi'an Jiaotong University, Xi'an, China and Yan Zheng, Department of Dermatology, the First Affiliated Hospital of Xi'an Jiaotong University, Xi'an, China. E-mail: wxiaofei@xjtu.edu.cn; zenyuan66@126.com

Cutaneous squamous cell carcinoma (cSCC), the second most common cancer in humans, has an estimated annual incidence of 1 million cases in the United States, with a rising trend (1, 2). Particularly in immunocompromised patients, cSCC tends to exhibit increased invasiveness (3). Investigating its molecular mechanisms holds crucial importance for disease treatment.

ATP citrate lyase (ACLY) is the first rate-limiting enzyme in the process of *de novo* lipogenesis, catalysing

SIGNIFICANCE

Cutaneous squamous cell carcinoma is a common skin tumour, and this study investigates the potential of ATP citrate lyase as a tumour biomarker and its role in cutaneous squamous cell carcinoma. The results revealed that ATP citrate lyase was upregulated in multiple human tumours and correlated with patient survival. ATP citrate lyase was elevated in both human cutaneous squamous cell carcinoma tissues and cell lines. Inhibiting ATP citrate lyase attenuated the malignant characteristics of tumour cells and the rate of tumour growth in animals. These findings indicate that ATP citrate lyase can serve as a tumour biomarker. Furthermore, it is highly expressed in cutaneous squamous cell carcinoma and promotes tumour progression.

the conversion of cytosolic citrate into acetyl-CoA and oxaloacetate, which can promote lipid synthesis. Studies have shown that most of the lipid in cancer cells comes from a *de novo* synthesis pathway (4, 5). Meanwhile, ACLY can promote a Warburg effect, thus promoting cancer metabolism and supporting cell growth. ACLY exerts an influence on the biological behaviour of tumour cells across various cancers, thereby impacting tumour progression. Inhibition of ACLY can induce mesenchymal to epithelial transformation in colon cancer cells (6). Elevated ACLY expression enhances the metastasis of breast cancer (7). Degradation of ACLY can inhibit proliferation and lipid synthesis in lung cancer cells (8). ACLY upregulation enhanced the proliferation and colony formation of endometrial cancer cells while inhibiting apoptosis. Additionally, nuclear-localized ACLY elevated histone acetylation levels, leading to the upregulation of genes associated with pyrimidine metabolism (9). However, its role in the development of cSCC has not been studied yet.

In this article, we employed bioinformatics to investigate the expression pattern of ACLY in tumours. Through immunohistochemistry, cellular experiments, and animal experiments, we explored the oncogenic role of ACLY in cSCC.

MATERIALS AND METHODS

ATP citrate lyase expression in cancers

Normal tissues were extracted from the Genotype-Tissue Expression (GTEx) database (<https://commonfund.nih.gov/GTEx/> data), and the Cancer Genome Atlas (TCGA) samples were

acquired from the University of California Santa Cruz (UCSC) Xena (<https://xenabrowser.net/datapages/>) website. We performed differential expression analysis using the "ggpubr" R package. The area under the curve (AUC) value of the receiver operating characteristic (ROC) curve was calculated using the "pROC" R package. The R package "ggplot2" was utilized to draw the bar plot. The 33 tumour abbreviations can be found in Appendix S1.

Prognostic value of ATP citrate lyase across cancers

Based on ACLY levels, TCGA pan-cancer samples were divided into 2 groups: high expression and low expression group (Fig. S1). Kaplan–Meier survival curves were established for disease-specific survival (DSS).

Correlation between ATP citrate lyase expression and immunological characteristics

TCGA cancer samples were classified into 6 immune subtypes, including C1 (wound healing), C2 (IFN- γ dominant), C3 (inflammatory), C4 (lymphocyte depleted), C5 (immunologically quiet), and C6 (TGF- β dominant). These 6 immune subtypes were identified based on 5 immune expression features, including macrophages/monocytes, overall lymphocyte infiltration, TGF- β response, IFN- γ response, and wound healing (10). In addition, we downloaded immune cell infiltration profiles from the Tumor Immune Estimation Resource (TIMER) database (<http://timer.cistrome.org/>) (11). TIMER algorithms were applied to analyse the correlation between infiltrated immune cells and ACLY expression.

Immunohistochemistry (IHC)

Fifteen normal samples and 36 cSCC samples were obtained from the Second Affiliated Hospital of Xi'an Jiaotong University. IHC was conducted following standard experimental procedures (12). The results were analysed according to the described method (13). The primary antibodies were as follows: ACLY (1:120, ab40793, Abcam, UK), c-Myc (1:150, GB13076, Servicebio, Hubei, China).

TUNEL

Paraffin-embedded tissue sections were stained using the Fluorescein (FITC) TUNEL Cell Apoptosis Detection Kit (G1502, Servicebio, China) according to the instructions.

Cell culture and transfection

Heka cells were isolated according to the described method (14) and cultured in keratinocyte medium (ScienCell, CA, USA). A431 cells were purchased from Procell (Wuhan, China). SCL-1 cells were purchased from Yobios Biotechnology (Xi'an, China). A431 and SCL-1 cells were cultured in Dulbecco's modified Eagle medium containing 10% foetal bovine serum. All the cells were maintained in a humidified incubator containing 5% CO₂ at 37°C.

The lentivirus and RNA duplexes were purchased from GenePharma (Shanghai, China). For RNA duplexes, the sequences were as follows: siACLY-1, 5'-GCACGAAGUCACAAUCUUUTT-3'; siACLY-2, 5'-GGCAUGUCCAACGAGCUCUAATT-3'; NC, 5'-UUCUCCGAACGUGUCACGUTT-3'. Transfection was performed using Lipofectamine™ RNAiMAX (Thermo, Waltham, MA, USA) and the final siRNA concentration was 12.5 nM. For lentivirus, the sh-ACLY sequence was: 5'-GGCATGTCCAACGAGCTCAA-3', and the sh-NC sequence was: 5'-TTCTCGAACGTGTACCGT-3'. Cells were infected with an MOI of

30, and selected with 5 μ g/mL puromycin for 2 weeks to obtain stable infected cell lines.

RNA extraction, cDNA synthesis, and quantitative real-time PCR

Total RNA was extracted using RNAiso Plus (9109, Takara, Kusatsu, Japan). Reverse transcription was performed using All-In-One 5X RT MasterMix (G490, abm, Vancouver, Canada), and quantitative real-time PCR was carried out using BlasTaq™ 2X qPCR MasterMix (G891, abm, Canada) on a Bio-Rad CFX96 system. Primers (Sangon Biotech, China) are described in Table S1.

Western blot

Human specimens were collected from 4 cSCC patients and 4 healthy samples. Proteins from tissues and cells were extracted following the described method and subsequently subjected to Western blot (15). The primary antibodies were as follows: ACLY (ab40793, Abcam, Cambridge, UK), c-Myc (T55150, Abmart, Shanghai, China), GAPDH (10494-1-AP, Proteintech, Rosemont, IL, USA), β -tubulin (M20005, Abmart, China), and β -actin (66009-1-Ig, Proteintech, USA).

CCK8 assay

After ACLY knockdown, cells were seeded in 96-well plates. Optical density (OD) values were detected at 450 nm after 24 hours, 48 hours, and 72 hours using a CCK8 solution (GK10001, Glpbio, Montclair, CA, USA) incubated with cells for 1.5 hours.

Flow cytometry

Transfected cells were collected and stained. Cell cycle analysis was performed using a DNA Content Quantitation Kit (CA1510, Solarbio, Beijing, China). Cell apoptosis analysis was conducted using the PE Annexin V Apoptosis Detection Kit (559763, BD Biosciences, San Jose, CA, USA), and caspase 3 activity in live cells was detected using the SuperView™ 488 Caspase-3 Assay Kit (40273ES, Yeasen, Shanghai, China). Measurements were carried out using a NovoCyte Flow Cytometer.

Animals and treatment

A total of 12 female nude mice aged 4–6 weeks were purchased from GemPharmatech (Jiangsu, China), divided into 4 groups: A431-sh-NC, A431-sh-ACLY, SCL-1-sh-NC, SCL-1-sh-ACLY. Tumour cells were injected into the dorsal region of nude mice. The length and width of the tumour was measured from the 6th day, and tumour volume was estimated using the formula $0.5 \times \text{length} \times \text{width} \times \text{width}$. On the 12th day, the nude mice were euthanized, and tumour mass was weighed. Ki67 and c-Myc expression levels in tumour tissues were assessed through IHC.

Statistical analysis

ACLY expression between the cancer group and normal group was compared using the Wilcoxon test. The Kruskal–Wallis test was used for immune subtype analysis. Spearman's test was performed to compare ACLY expression and immune infiltration. All experiments were performed in biological triplicate. Prism GraphPad (version 8.0; www.graphpad.com) was used for statistical analysis, and data are expressed as the mean \pm standard deviation. One-way ANOVA or two-way ANOVA was used to compare the differences between the siRNA group and the control group. Student's *t*-test was used to compare the differences between the sh-ACLY group and sh-NC group. A threshold of $p < 0.05$ was considered statistically significant.

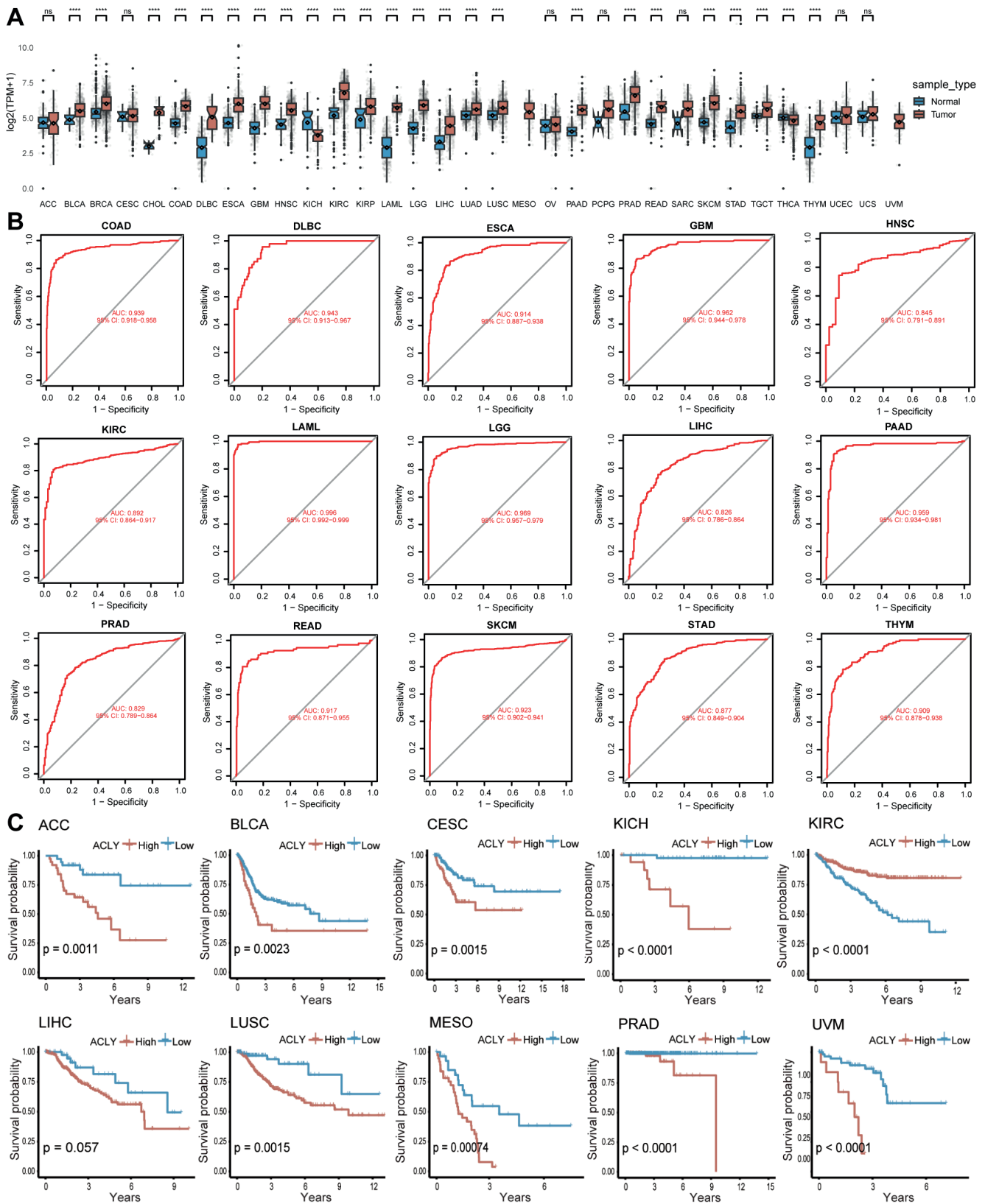


Fig. 1. ATP citrate lyase (ACLY) expression pattern across cancers. (A) ACLY expression based on normal data from GTEx and tumour data from TCGA. (B) The diagnostic value of ACLY. (C) Kaplan-Meier curves of ACLY across cancers. The 33 tumour abbreviations can be found in Appendix S1. * $p < 0.05$, ** $p < 0.01$, *** $p < 0.001$, **** $p < 0.0001$, vs normal control.

RESULTS

ATP citrate lyase can serve as a general tumour biomarker

As shown in **Fig. 1A**, ACLY was differentially expressed in 24 tumours. Among them, ACLY was highly expressed in 22 cancer types and expressed at low levels in KICH and THCA. ROC curves reflected a good diagnostic ability of ACLY for various types of cancer (Fig. 1B). To eliminate the influence of deaths caused by factors other than disease, we analysed DSS rather than overall survival (OS). Kaplan–Meier survival analysis (Fig. 1C) showed that patients with high ACLY expression had a worse prognosis in ACC, BLCA, CESC, KICH, LIHC, LUSC, MESO, PRAD, and UVM. In summary, we found that ACLY was dysregulated in a variety of cancers and was correlated with prognosis. It may serve as a diagnostic marker, holding significance for the occurrence and development of tumours.

ATP citrate lyase was associated with the immunological characteristics of tumours

ACLY expression differed in immune subtype in 17 types of cancer (**Fig. 2A**). For most tumours, ACLY was highest in the C1 or C4 subtype and lowest in the C3

subtype. We used TIMER algorithm to analyse immune infiltration. As displayed in Fig. 2B, ACLY was correlated with immune cell abundance in a variety of cancers. The correlation between ACLY and macrophages was the closest. Besides, ACLY was significantly correlated with a variety of immune cells in BRCA, CHOL, HNSC, KIRC, KICH, KIRP, LIHC, PRAD, and THCA. These results indicate a significant impact of ACLY on tumour immune cell infiltration.

ATP citrate lyase was elevated in cutaneous squamous cell carcinoma

A total of 36 cSCC tissues and 15 healthy control specimens were collected. IHC staining revealed weak expression of ACLY in the normal epidermis and strong expression in almost all tumour cells. In normal epidermis, ACLY was confined to the basal layer and exclusively expressed in the cytoplasm. However, in cSCC, ACLY was expressed in both the cytoplasm and the cell nucleus (**Fig. 3A**). We also confirmed the increased expression of ACLY in human cSCC tissues by Western blot (Fig. 3B). Moreover, at both mRNA and protein levels, ACLY was upregulated in A431 and SCL-1 cells compared with Heka cells (Fig. 3C–D).

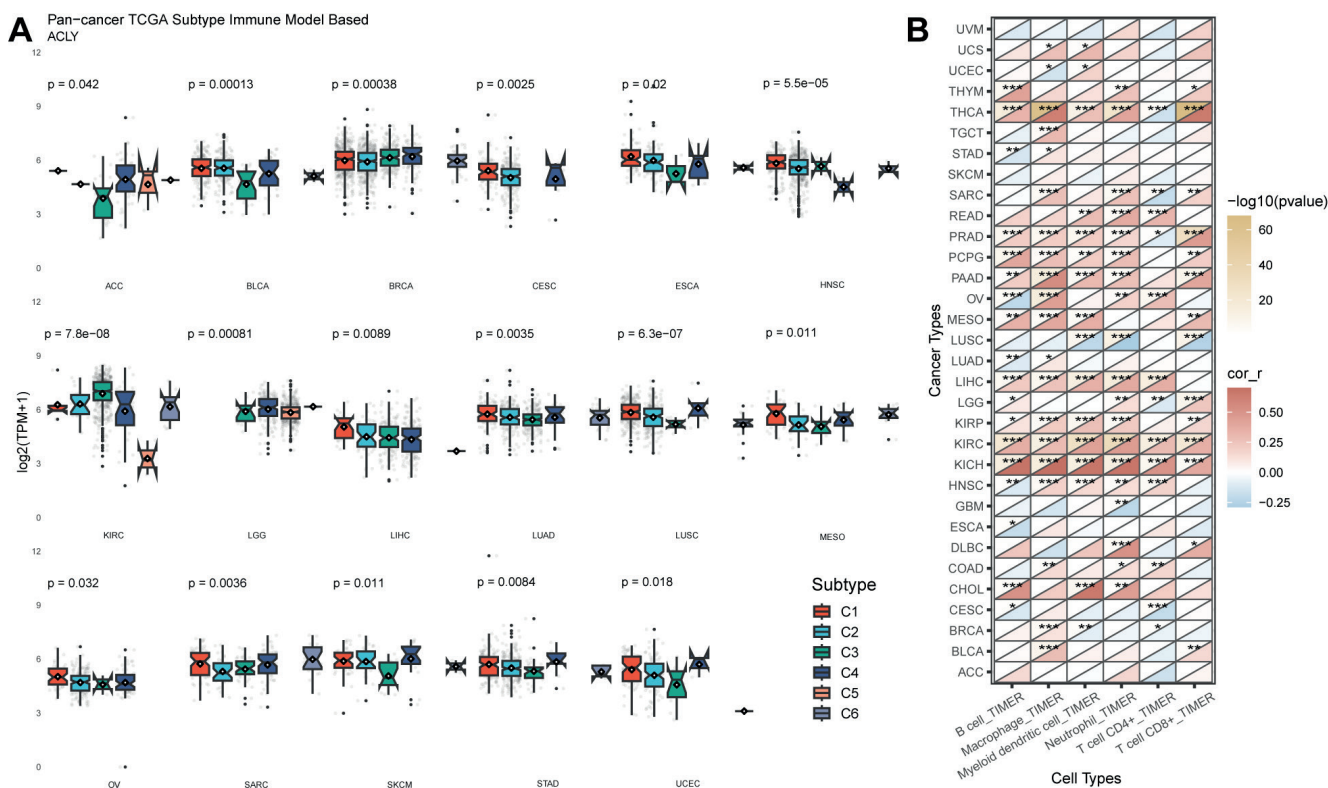


Fig. 2. Association between ATP citrate lyase (ACLY) expression and immunological characteristics. (A) ACLY expression in different immune subtypes. C1 (wound healing), C2 (IFN- γ dominant), C3 (inflammatory), C4 (lymphocyte depleted), C5 (immunologically quiet), and C6 (TGF- β dominant). (B) Correlation between ACLY expression and immune-infiltrating cells based on the TIMER algorithm. The 33 tumour abbreviations can be found in Appendix S1. * $p < 0.05$, ** $p < 0.01$, *** $p < 0.001$.

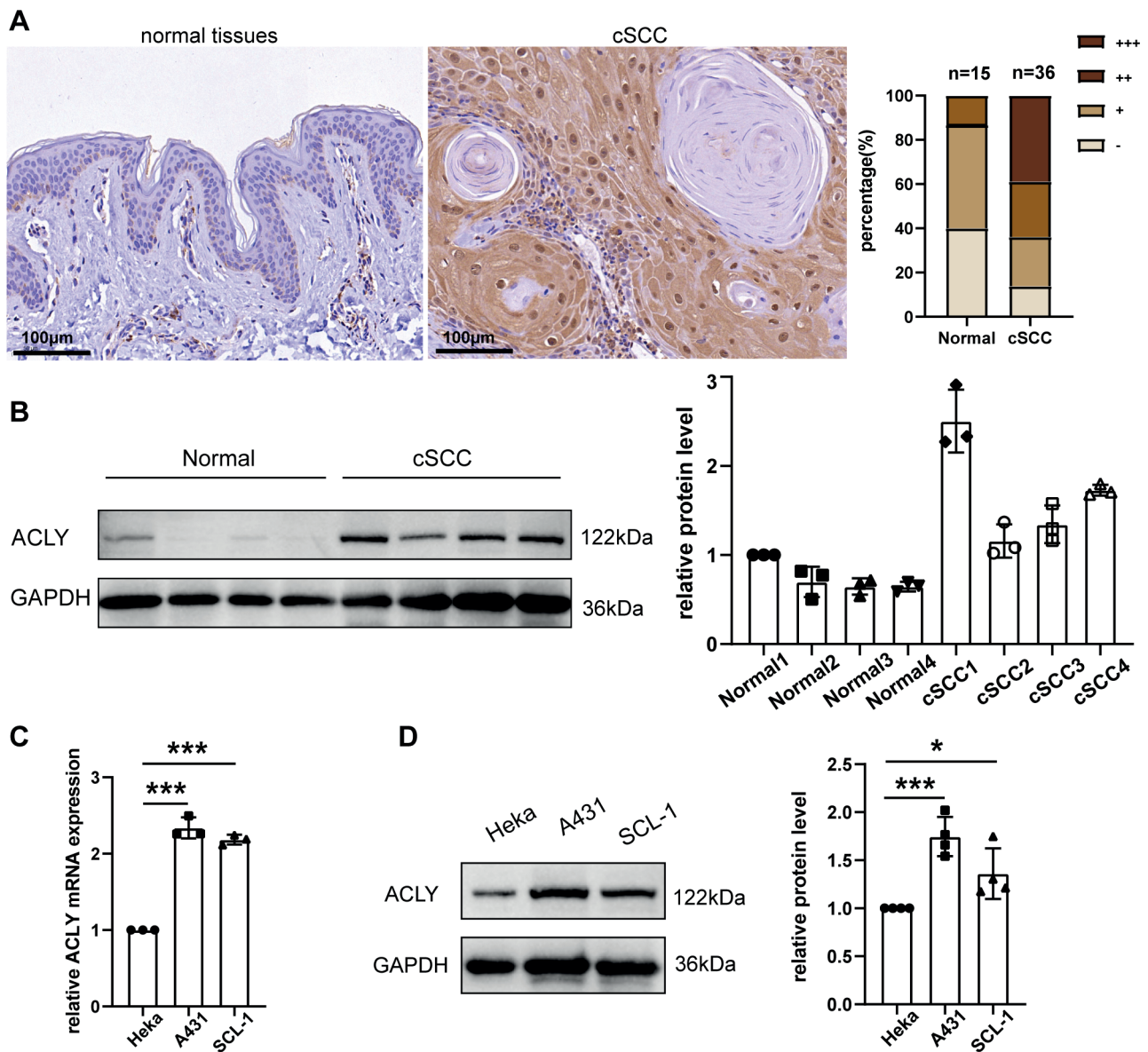


Fig. 3. Elevated ATP citrate lyase (ACLY) expression in cSCC. (A) ACLY IHC staining in normal skin and cSCC samples. (B) Protein levels of ACLY in normal skin and cSCC tissues. (C) qRT-PCR analysis of ACLY in Heka and cSCC cells ($N=3$). (D) Western blot analysis of ACLY in Heka and cSCC cells ($N=4$). * $p < 0.05$, *** $p < 0.001$, vs Heka.

ATP citrate lyase silencing inhibited cell proliferation and induced apoptosis

To establish an ACLY low expression model, we transfected cSCC cells with siRNA and assessed the knockdown efficiency using qRT-PCR (Fig. 4A) and Western blot (Fig. 4B). Cells with reduced ACLY levels exhibited a slower growth rate (Fig. 4C), along with G1 phase arrest (Fig. 4D). We subsequently examined cell apoptosis by flow cytometry. The results suggested that apoptosis of tumour cells increased to varying degrees after ACLY knockdown (Fig. 4E). Simultaneously, intracellular caspase-3 activity was elevated (Fig. 4F). Besides, we observed a decrease in the mRNA levels of key enzymes in lipid synthesis, including ACACA, FASN, and SCD1,

following ACLY silencing (Fig. S2A). Furthermore, Hallmark enrichment analysis of ACLY indicated that the Myc pathway was one of the widely enriched pathways (Fig. S3), and the protein levels of c-Myc were downregulated following ACLY knockdown (Fig. 4G). These results indicate that inhibiting ACLY can alleviate the malignant behaviour of cSCC cells.

ATP citrate lyase knockdown suppressed tumour growth in vivo

When using siRNA to knock down genes, the effects typically last for a relatively short duration. However, following lentivirus infection and subsequent puromycin selection, stable cell lines with low ACLY expression

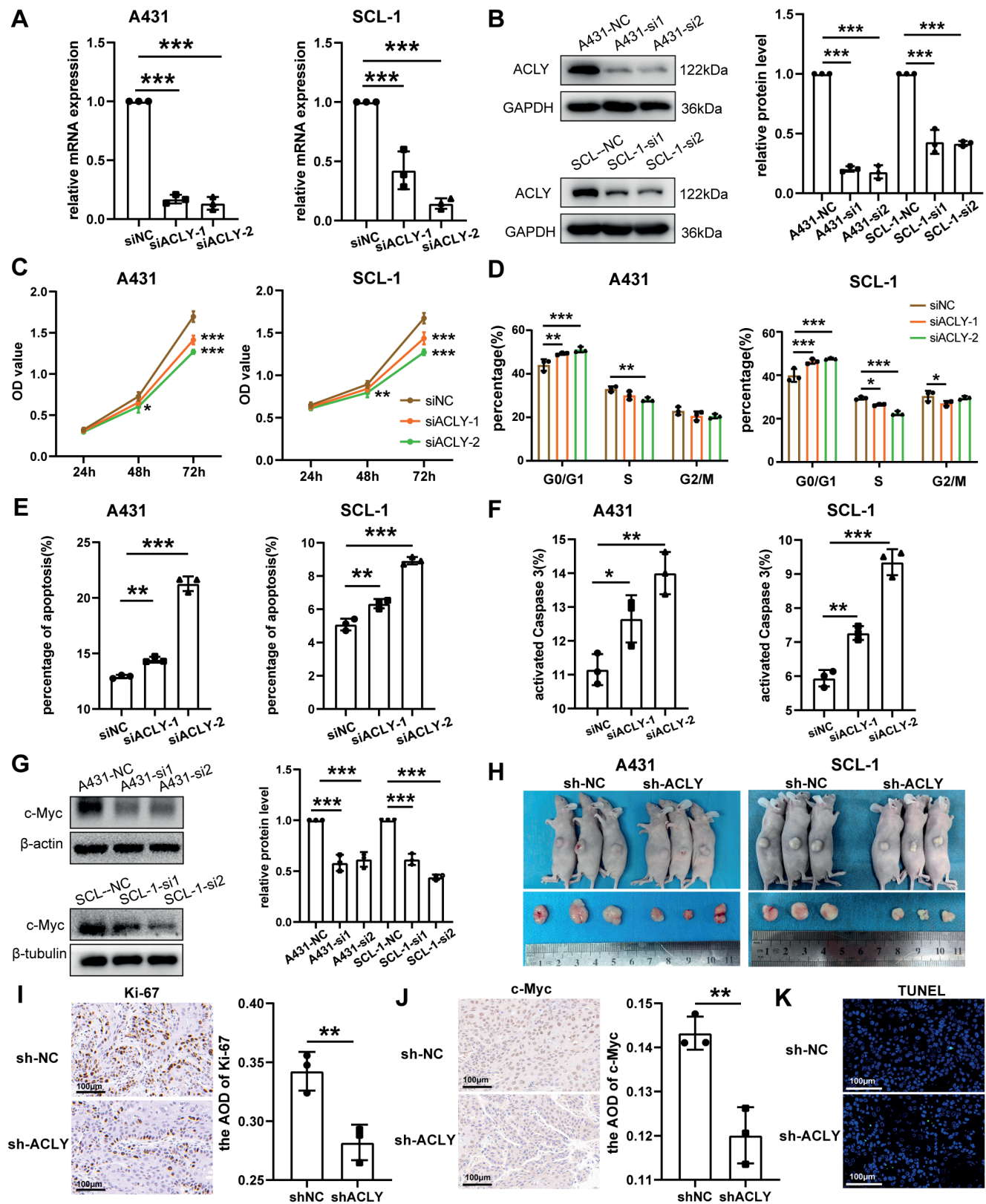


Fig. 4. Effects of ATP citrate lyase (ACLY) knockdown on cutaneous squamous cell carcinoma (cSCC). (A–B) qRT-PCR and Western blot analysis of ACLY knockdown efficiency in A431 and SCL-1 cells ($N=3$). (C) Growth rate of cSCC cells after ACLY knockdown. (D) Cell cycle of cSCC cells after ACLY knockdown ($N=3$). (E) Flow cytometry analysis of cell apoptosis rate after ACLY knockdown ($N=3$). (F) Flow cytometry analysis of caspase 3 activity after ACLY knockdown ($N=3$). (G) Western blot detection of c-Myc level ($N=3$). (H) Subcutaneous tumour display in nude mice on day 12 ($N=3$). (I) IHC detection of Ki67 expression in tumour tissues ($N=3$). (J) IHC detection of c-Myc expression in tumour tissues ($N=3$). (K) TUNEL staining in tumour tissues ($N=3$). Quantitative data are presented as the mean and standard deviation (SD). * $p < 0.05$, ** $p < 0.01$, *** $p < 0.001$, vs normal control.

can be obtained. Subsequently, these cells were subcutaneously implanted in nude mice to assess the impact of ACLY knockdown on the growth of tumour tissues. As shown in Fig. 4H and Fig. S2B, the growth rate of tumour tissues decreased, leading to a reduction in volume after knockdown. In Fig. S2C, the tumour mass in the sh-ACLY group was notably lower than that in the sh-NC group. Additionally, IHC revealed a significant decrease in Ki-67 (Fig. 4I) and c-Myc (Fig. 4J) expression in the sh-ACLY group. The tumour tissue TUNEL fluorescence increased in the sh-ACLY group, representing an increase in cell apoptosis (Fig. 4K). These findings indicate that ACLY knockdown exerts inhibitory effects on tumour growth.

DISCUSSION

Our findings demonstrated that ACLY was upregulated in most cancer types, consistent with previous studies reporting its high expression in glioblastoma (16), non-small cell lung cancer (17) and clear cell renal carcinoma (18). Besides, an analysis of the GEO database (GSE9115 and GSE126698) showed that ACLY was upregulated in anaplastic thyroid cancer (ATC) (19). High ACLY expression was usually associated with poor prognosis. This observation aligns with studies reporting better OS in acute myeloid leukaemia patients with low ACLY expression (20), as well as the association between ACLY positivity and poor OS in node-negative non-small cell lung cancer patients (21). In addition, high ACLY expression has been linked to poor prognosis in prostate cancer (22). These studies support our conclusion that ACLY is elevated and exhibits high diagnostic value in multiple cancers.

Tumour immune infiltrate cells are closely related to tumour development. ACLY was predominantly expressed in the C1 or C4 subtype across most types. The C1 subtype is typically characterized by a high cell proliferation rate, while the C4 subtype signifies a lack of lymphocytes in the tumour microenvironment (10). Generally, C3 has the best prognosis, while C1 and C4 subtypes are associated with poorer outcomes (10). This can explain the association of ACLY and worse clinical outcomes in most tumours. In both the mouse HCC model and human HCC tissues, inhibition of ACLY results in an increase in CD8⁺ T cells, indicating that ACLY affects immune cell infiltration around the tumour (23). This further emphasizes the association of ACLY with the immunological characteristics of tumours. Our subsequent studies will focus on experimental investigations into the role of ACLY in the tumour microenvironment.

We declared that ACLY was also highly expressed in cSCC. In cancer cells, high ACLY expression is essential for maintaining high cell proliferation rates and

supporting lipid synthesis required for rapid growth. ACLY promotes the Warburg effect in cancer cells by depleting cytoplasmic citrate and enhancing phosphofructokinase 1 (PFK1) activity, leading to increased glycolysis (24).

Our *in vitro* studies indicated that ACLY inhibition hinders cell proliferation, induces cell cycle arrest, and promotes apoptosis in tumour cells. Furthermore, our animal experiments confirmed the same results. Consistent with our research, ACLY inhibition has been shown to impede cell proliferation and induce cell apoptosis in melanoma (25), and lung adenocarcinoma (17, 26, 27). We also observed a reduction in the mRNA levels of ACACA, FASN, and SCD1 in cSCC cells after ACLY knockdown. ACLY transforms citrate into acetyl-CoA, and ACACA produces malonyl-CoA from acetyl-CoA. FASN facilitates the elongation of fatty acid chains using the malonyl scaffold, whereas SCD monosaturates long chain fatty acids (28). Furthermore, our *in vivo* and *in vitro* studies also indicated a decrease in c-Myc expression after ACLY silencing. c-Myc has long been a mysterious oncogene, as it affects nearly all cellular processes (28). Aberrant upregulation of c-Myc is observed in many cancers, leading to excessive cell proliferation and survival, thereby promoting cancer progression, making it a key focus in cancer research (29). Our Hallmark enrichment and Western blot results suggested a close association between ACLY and c-Myc, indicating that ACLY is a gene closely related to various tumour processes, such as cell metabolism and cell cycle. These findings further emphasize the significant potential of ACLY as a target for cSCC and warrant further investigation.

Our study provides a comprehensive insight into the expression pattern of ACLY in various cancer types, suggesting it can serve as a tumour biomarker. Furthermore, ACLY is upregulated in cSCC, and functional experiments further support its role in promoting cancer cell proliferation, highlighting its possibility as a therapeutic target.

ACKNOWLEDGEMENTS

The authors would like to thank Mr Zhihu Zheng (Department of Urology, the First Affiliated Hospital of Xi'an Jiaotong University) for tissue collection assistance after circumcision.

This work was supported by a grant from the National Natural Science Foundation of China (82273541).

This study has been approved by the Biomedical Ethics Committee of Xi'an Jiaotong University Health Science Center. Informed consent was obtained from all patients before collecting specimens.

The data used in this study are available in the Cancer Genome Atlas (TCGA), Genotype-Tissue Expression (GTEx) database, and Tumor Immune Estimation Resource (TIMER). Other experimental data are available from the corresponding author on reasonable request.

The authors have no conflicts of interest to declare.

REFERENCES

1. Corchado-Cobos R, Garcia-Sancha N, Gonzalez-Sarmiento R, Perez-Losada J, Canueto J. Cutaneous squamous cell carcinoma: from biology to therapy. *Int J Mol Sci* 2020; 21: 2956.
2. Chang MS, Azin M, Demehri S. Cutaneous squamous cell carcinoma: the frontier of cancer immunoprevention. *Annu Rev Pathol* 2022; 17: 101–119.
3. Manyam BV, Garsa AA, Chin RI, Reddy CA, Gastman B, Thorstad W, et al. A multi-institutional comparison of outcomes of immunosuppressed and immunocompetent patients treated with surgery and radiation therapy for cutaneous squamous cell carcinoma of the head and neck. *Cancer* 2017; 123: 2054–2060.
4. Menendez JA, Lupu R. Fatty acid synthase and the lipogenic phenotype in cancer pathogenesis. *Nat Rev Cancer* 2007; 7: 763–777.
5. Rohrig F, Schulze A. The multifaceted roles of fatty acid synthesis in cancer. *Nat Rev Cancer* 2016; 16: 732–749.
6. Ascencao K, Dilek N, Augsburg F, Panagaki T, Zuhra K, Szabo C. Pharmacological induction of mesenchymal-epithelial transition via inhibition of H2S biosynthesis and consequent suppression of ACLY activity in colon cancer cells. *Pharmacol Res* 2021; 165: 105393.
7. Adorno-Cruz V, Hoffmann AD, Liu X, Dashzeveg NK, Taftaf R, Wray B, et al. ITGA2 promotes expression of ACLY and CCND1 in enhancing breast cancer stemness and metastasis. *Genes Dis* 2021; 8: 493–508.
8. Zhang C, Liu J, Huang G, Zhao Y, Yue X, Wu H, et al. Cullin3-KLHL25 ubiquitin ligase targets ACLY for degradation to inhibit lipid synthesis and tumor progression. *Genes Dev* 2016; 30: 1956–1970.
9. Dai M, Yang B, Chen J, Liu F, Zhou Y, Zhou Y, et al. Nuclear-translocation of ACLY induced by obesity-related factors enhances pyrimidine metabolism through regulating histone acetylation in endometrial cancer. *Cancer Lett* 2021; 513: 36–49.
10. Thorsson V, Gibbs DL, Brown SD, Wolf D, Bortone DS, Ou Yang TH, et al. The immune landscape of cancer. *Immunity* 2018; 48: 812–830 e814.
11. Li T, Fan J, Wang B, Traugh N, Chen Q, Liu JS, et al. TIMER: A web server for comprehensive analysis of tumor-infiltrating immune cells. *Cancer Res* 2017; 77: e108–e110.
12. Pinheiro C, Longatto-Filho A, Scapulatempo C, Ferreira L, Martins S, Pellerin L, et al. Increased expression of monocarboxylate transporters 1, 2, and 4 in colorectal carcinomas. *Virchows Arch* 2008; 452: 139–146.
13. Jia J, Li C, Luo S, Liu-Smith F, Yang J, Wang X, et al. Yes-associated protein contributes to the development of human cutaneous squamous cell carcinoma via activation of RAS. *J Invest Dermatol* 2016; 136: 1267–1277.
14. Johansen C. Generation and culturing of primary human keratinocytes from adult skin. *J Vis Exp* 2017; 130: 56863.
15. Li C, Xiao L, Jia J, Li F, Wang X, Duan Q, et al. Cornulin is induced in psoriasis lesions and promotes keratinocyte proliferation via phosphoinositide 3-kinase/Akt pathways. *J Invest Dermatol* 2019; 139: 71–80.
16. Beckner ME, Fellows-Mayle W, Zhang Z, Agostino NR, Kant JA, Day BW, et al. Identification of ATP citrate lyase as a positive regulator of glycolytic function in glioblastomas. *Int J Cancer* 2010; 126: 2282–2295.
17. Migita T, Narita T, Nomura K, Miyagi E, Inazuka F, Matsuura M, et al. ATP citrate lyase: activation and therapeutic implications in non-small cell lung cancer. *Cancer Res* 2008; 68: 8547–8554.
18. Teng L, Chen Y, Cao Y, Wang W, Xu Y, Wang Y, et al. Overexpression of ATP citrate lyase in renal cell carcinoma tissues and its effect on the human renal carcinoma cells in vitro. *Oncol Lett* 2018; 15: 6967–6974.
19. Huang SS, Tsai CH, Kuo CY, Li YS, Cheng SP. ACLY inhibitors induce apoptosis and potentiate cytotoxic effects of sorafenib in thyroid cancer cells. *Endocrine* 2022; 78: 85–94.
20. Wang J, Ye W, Yan X, Guo Q, Ma Q, Lin F, et al. Low expression of ACLY associates with favorable prognosis in acute myeloid leukemia. *J Transl Med* 2019; 17: 149.
21. Osugi J, Yamaura T, Muto S, Okabe N, Matsumura Y, Hoshino M, et al. Prognostic impact of the combination of glucose transporter 1 and ATP citrate lyase in node-negative patients with non-small lung cancer. *Lung Cancer* 2015; 88: 310–318.
22. Zhang Q, Yin X, Pan Z, Cao Y, Han S, Gao G, et al. Identification of potential diagnostic and prognostic biomarkers for prostate cancer. *Oncol Lett* 2019; 18: 4237–4245.
23. Xiang W, Lv H, Xing F, Sun X, Ma Y, Wu L, et al. Inhibition of ACLY overcomes cancer immunotherapy resistance via polyunsaturated fatty acids peroxidation and cGAS-STING activation. *Sci Adv* 2023; 9: eadi2465.
24. Icard P, Wu Z, Fournel L, Coquerel A, Lincet H, Alifano M. ATP citrate lyase: a central metabolic enzyme in cancer. *Cancer Lett* 2020; 471: 125–134.
25. Guo W, Ma J, Yang Y, Guo S, Zhang W, Zhao T, et al. ATP-citrate lyase epigenetically potentiates oxidative phosphorylation to promote melanoma growth and adaptive resistance to MAPK inhibition. *Clin Cancer Res* 2020; 26: 2725–2739.
26. Hatzivassiliou G, Zhao F, Bauer DE, Andreadis C, Shaw AN, Dhanak D, et al. ATP citrate lyase inhibition can suppress tumor cell growth. *Cancer Cell* 2005; 8: 311–321.
27. Hanai J, Doro N, Sasaki AT, Kobayashi S, Cantley LC, Seth P, et al. Inhibition of lung cancer growth: ATP citrate lyase knockdown and statin treatment leads to dual blockade of mitogen-activated protein kinase (MAPK) and phosphatidylinositol-3-kinase (PI3K)/AKT pathways. *J Cell Physiol* 2012; 227: 1709–1720.
28. Stine ZE, Walton ZE, Altman BJ, Hsieh AL, Dang CV. MYC, metabolism, and cancer. *Cancer Discov* 2015; 5: 1024–1039.
29. Dhanasekaran R, Deutzmann A, Mahauad-Fernandez WD, Hansen AS, Gouw AM, Felsher DW. The MYC oncogene: the grand orchestrator of cancer growth and immune evasion. *Nat Rev Clin Oncol* 2022; 19: 23–36.